Fluid flow and deformation

M.Geo.239
30 Jan 2019

Elco Luijendijk
eluijen@gwdg.de

Faults and fluid flow

- Lecture 10: Effect of faults on fluid flow
  - Permeability structure of faults
  - Fluid flow in faults: models and field evidence
- However, how did faults & fractures get there in the first place?
- This lecture: Effects of fluid flow & pressure on deformation
  - Deformation and pore pressure
  - Brief overview of fluids & deformation case studies
- = bonus lecture: only max. 1 very general question about this at the exam

Review of effective stress

- Effective stress is a function of the total stress and the fluid pressure. Note that alpha equals 1 in almost all cases

$$\sigma_e = \sigma_t - \alpha P_f$$

- The total stress is the weight of the overburden, which includes the weight of the rock matrix and the pore fluid and is a function of porosity (ϕ), density (ρ), and depth (d)

$$\sigma_t = (1-\phi)\rho_r g d - \phi \rho_f g d$$

- Fluid pressure acts in all directions -> effective stress also works in three dimensions / the three principal stress directions:
- If the fluid pressure is equal to the total stress effective stress is zero, and fluid pressure is defined as lithostatic.
- If effective stress is negative: tensile failure of rocks with no offset

$$\sigma_{e,1} = \sigma_{t,1} - \alpha P_f$$
$$\sigma_{e,2} = \sigma_{t,2} - \alpha P_f$$
$$\sigma_{e,3} = \sigma_{t,3} - \alpha P_f$$

Fracturing rocks

- However, deformation by tensile failure is not the only mechanism of deformation: rocks can also deform by shear failure

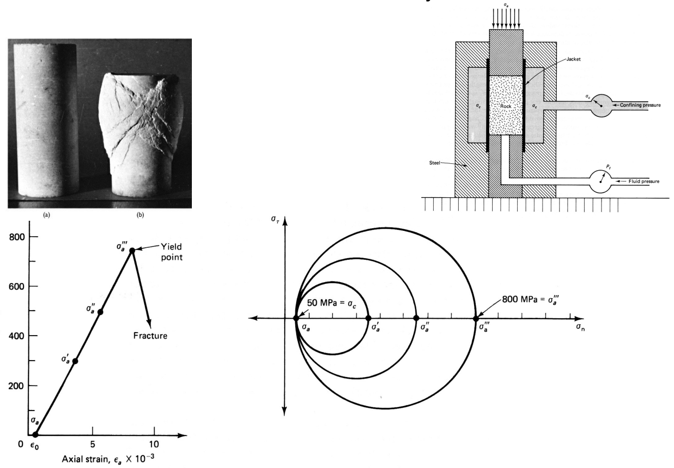

Fracturing rocks

- Representation of stress with Mohr circles:

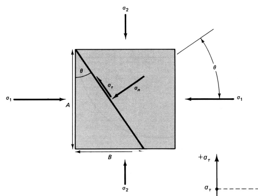

$$\sigma_n = \left(\frac{\sigma_1 + \sigma_2}{2}\right) + \left(\frac{\sigma_1 - \sigma_2}{2}\right) \cos 2\theta$$

$$\sigma_\tau = \left(\frac{\sigma_1 - \sigma_2}{2}\right) \sin 2\theta$$

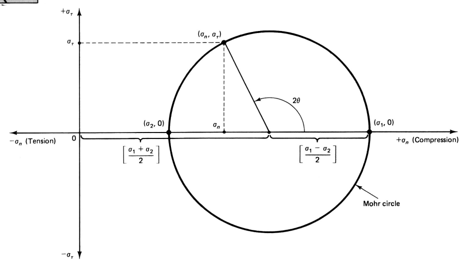

Fracturing rocks

- Shear failure is a function of the differential stress = the difference between the maximum and minimum stress, σ1 - σ3
- The larger the differential stress, the larger the Mohr circle, and the higher the chance that the Mohr-Couloumb failure criterion is reached (ie the circle touches the line)
- Coulomb's law of failure: $\tau = \tau_0 + \sigma_n tan\phi$
- τ0 is the shear resistance of a cohesive material, σn is the normal stress on the plane, ϕ is the angle of internal friction, which is 30˚ for most materials
- -> most materials start to develop fracture oriented at 30 degrees to the compressive stress

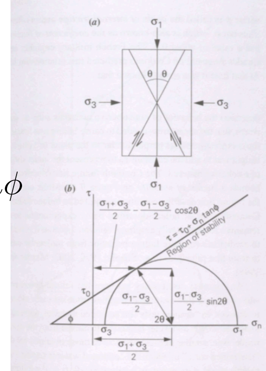

Figure 9.2. (a) Relation between principal stresses and fractures in a sample brought to failure in a *triaxial test* and (b) representation of the failure conditions on a *Mohr diagram*.

Ingebritsen et al. (2006) Groundwater in geologic processes

Fracturing rocks

- Coefficient of friction (tan ϕ) is typically 0.6 and varies between 0.5 and 0.85 for most rocks
- Note that the lower the coefficient of friction, the flatter the failure envelope becomes in the graph on the right -> the weaker the rock and the higher the chance of failure

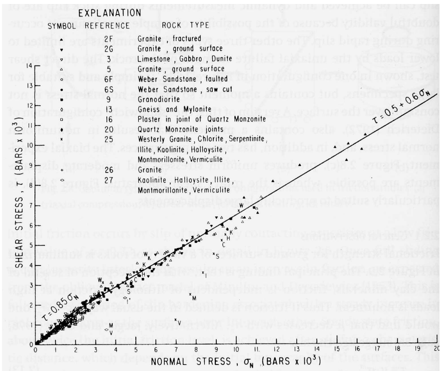

Fig. 2.9. Frictional strength for a wide variety of rocks plotted as a function of normal load. The lettered data points refer to clay minerals as indicated in the key. (From Byerlee, 1978.)

Fracturing rocks

- Example of fracture strength of rocks from lab experiments:

$$\sigma_\tau = S_o + \mu\sigma_n$$

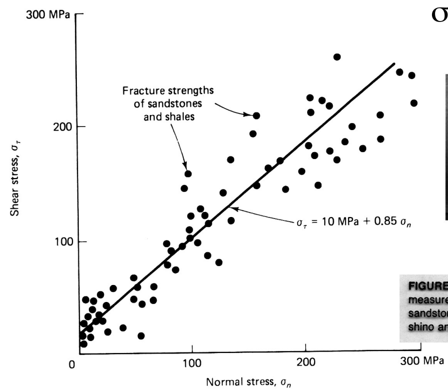

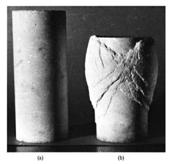

FIGURE 5–6 Summary of laboratory measurements of fracture strength of sandstone and shale. (Data from Hoshino and others, 1972.)

Fracturing rocks

- Two kinds of fractures:
  - shear fractures -> faults
  - tensile fractures -> joints

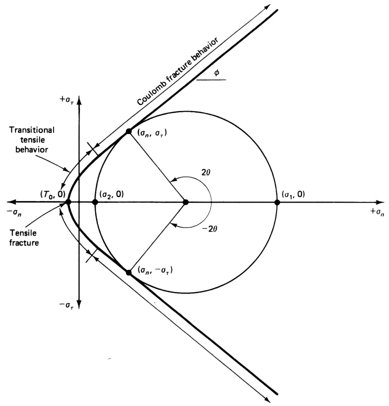

FIGURE 5–5 Three fields of the fracture, or Mohr, envelope. The tensile field shows a fixed strength, T_0. The Coulomb fracture field shows a linear increase in shear strength, σ_τ, with normal stress, σ_n, and a slope tan ϕ. The two points of tangency of the Mohr circle represent the states of stress on the two planes whose normals are θ from the σ_1-axis (Fig. 3-23). Transitional-tensile behavior is transitional between tensile and Coulomb fracture.

Fractures & fluid pressure

- Tests with dry, drained and undrained rocks showed a strong difference between the strenght of drained and undrained rocks
- Can be resolved by using effective stress instead of total stress
- -> fluid pressure strongly affects shear & tensile failure in the subsurface, the higher the fluid pressure the higher the chance of failure

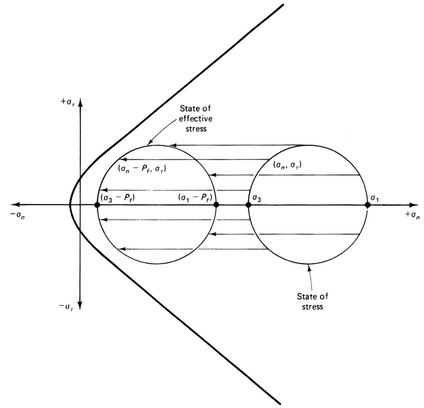

Fractures and fluid pressures

- Example of three different ways to get a fracture moving:

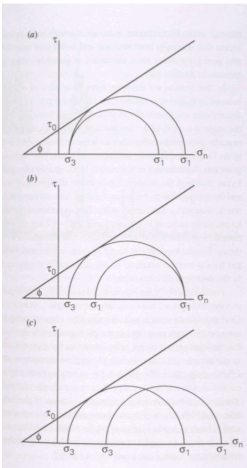

Figure 9.3. Mohr diagrams showing failure conditions induced by (a) increasing the greatest principal stress σ_1, (b) decreasing the least principal stress σ_3, and (c) increasing the internal pore-fluid pressure P_f. In each case the σ_1 and σ_3 values plotted on the abscissa are actually the effective stresses, that is, $\sigma_1 - P_f$ and $\sigma_3 - P_f$.

Ingebritsen et al. (2006) Groundwater in geologic processes

Fault stress in the upper crust

- Results from stress & hydraulic conductivity data from deep boreholes in the western US:
- Most fault appear to be close to failure
- Most of the crust may be critically stressed (ie a small push will induce failure of these faults)

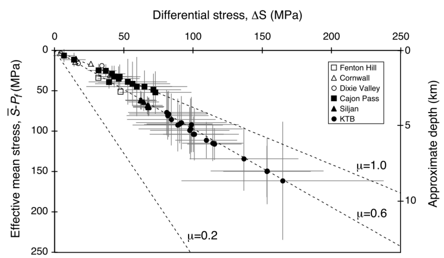

Figure 1. Dependence of differential stress, ΔS, on effective mean stress, $\bar{S} - P_f$, at six locations where deep stress measurements have been made. Dashed lines illustrate relationships predicted using Coulomb frictional-failure theory for various coefficients of friction, μ. References: Fenton Hill—Barton et al. (1988); Cornwall—Pine et al. (1983), Batchelor and Pine (1986); Dixie Valley—Hickman et al. (1997); Cajon Pass—Zoback and Healy (1992); Siljan—Lund and Zoback (1999); KTB (German Continental Deep Drilling Program)—Brudy et al. (1997).

Townend and Zoback (2000) Geology

Fault stress in the upper crust

- Hydraulically conductive fractures are those optimally oriented for frictional sliding
- Pore pressure is quasi hydrostatic down to a depth of 10km, probably due to percolation along critically stressed fractures,
- The crust is at the critical stress level for frictional sliding of faults with μ ~0.6, similar to laboratory derived values.
- This mechanisms maintains high effective stresses in the upper crust which can then sustain most of the plate driving tectonic forces.
- Is most of the crust 'critically stressed'? ie is only a small push needed to get most faults moving?

Figure 3. Shear and normal stresses on fractures identified with borehole imaging techniques in Cajon Pass (triangles), Long Valley (circles), and Nevada Test Site (squares) boreholes. Filled symbols represent hydraulically conductive fractures and faults, and open symbols represent nonconductive fractures. Original data are from Barton et al. (1995).

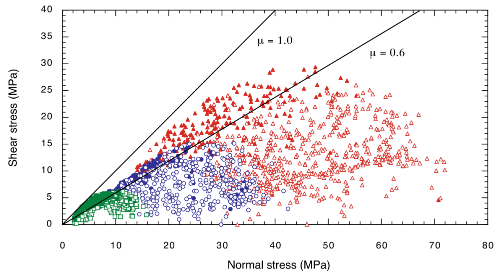

Townend and Zoback (2000) Geology

Effects of fluids on fault strength

- Fluid pressure is not the only control of fluids on fault strength:
- The formation of authigenic clays decreases fault strength
- See low values of coefficients of friction in diagram on the right:

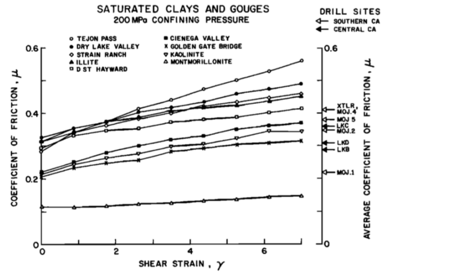

Fig. 11. The coefficient of friction as a function of shear strain for saturated gouges and pure clays under 200-MPa confining pressure. The strain axis begins at the 'elbow' of the associated strength in curves in Figure 10 to distinguish initial compaction from shear strain. For comparison of laboratory and field measurements, the far right of the figure shows friction data for southern and central California drill sites as determined by hydrofracturing techniques [*Zoback et al.*, 1980]. Arrows indicate the average coefficients of friction (±0.06) from stress measurements at several depths.

Morrow et al (1982) Coefficient of friction for various clay gouge samples from the San Andreas fault

Effects of fluids on fault strength

- Adsorbed water strongly modifies the strength of fault gouge minerals
- Depends on many factors: fluid chemistry, pH, temperature and pressure
- Most/all faults zones have sufficient fluids to change the strength of fault gouge….

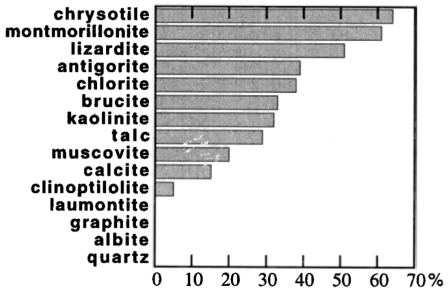

Figure 3. Percentage decrease in frictional strength of gouge minerals after saturation.

Morrow (2000) GRL

Pore pressure & deformation

- Case study from mt. Hood in the Cascades in Oregon (western US)
- Volcanic area near the coast with high rainfall and high groundwater recharge rates (1.5 m per year) with a high seasonal variability
- Concentrated seismic activity ~5 km beneath the mountain

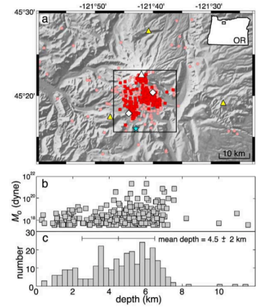

Fig. 1. (a) Shaded relief map of Mt. Hood, Oregon, indicating all earthquakes (pink circles and red squares) and selected (for criteria see text) earthquakes (red squares), stream discharge gauging station on Salmon River (blue star), summit of Mt. Hood (large white triangle), and hydrothermal Swim Warm Springs (western white diamond) and Meadows Spring (eastern white diamond). Three (small yellow triangles) out of 14 relevant seismometers (Appendix A) are located within the map region. (b) Seismic moment, M_o, versus earthquake depth. (c) Histogram of earthquake depths, mean earthquake depth (4.5 km), and range of 1σ standard deviation (2 km).

Saar & Manga (2003) EPSL

Pore pressure & deformation

- Seismic activity fluctuates over time, and shows a seasonal trend
- link = additional fluid mass -> increase in normal stress on critically stressed faults -> increasing chance of failure and seismic activity
- The time lag is due to the diffusion of pore pressure, which is a function of permeability and storativity

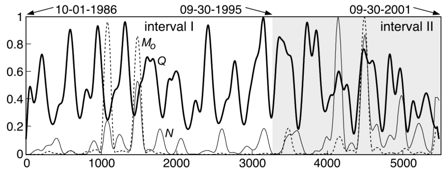

Fig. 7. Interpolated time series from Fig. 6, normalized by each series' absolute maximum value. Local maxima of number of earthquakes (thin solid line) and seismic moment (thin dashed line) typically follow local maxima of stream discharge (bold solid line) after a time lag of about 151 days.

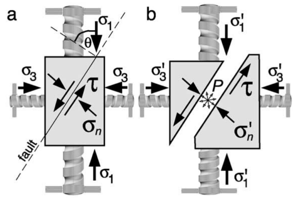

Time series of seasonal groundwater recharge and seismic activity (top) and conceptual model of fluid pressure in faults (bottom)
Saar & Manga (2003) EPSL

Groundwater pumping, uplift & seismicity

- Strong uplift in parts of California around the San Joaquin Valley as recorded by GPS data
- And very high rates of pumping: up to 120 m decrease on groundwater level in 100 years
- Could these two effects be related?

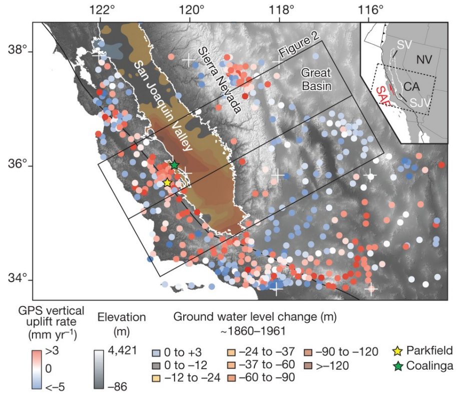

Amos et al. (2014) Nature 509

Groundwater pumping, uplift & seismicity

- Decrease in groundwater level: decrease in load on the crust
- Generates a flexural response: less weight, the lithosphere flexes upward
- Due to the flexural rigidity, the uplift is not confined to the San Joaquin Valley only, but also affects the adjacent areas:

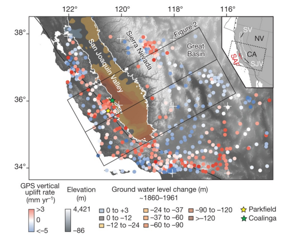

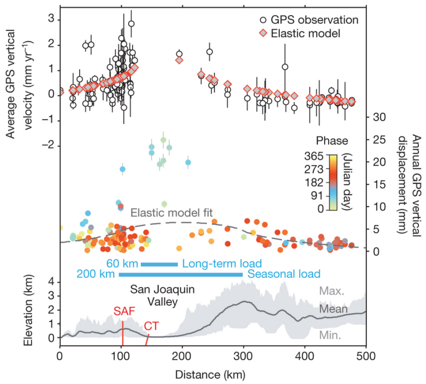

Amos et al. (2014) Nature 509

Groundwater pumping, uplift & seismicity

- Additional argument for groundwater pumping indiced uplift: strong seasonal signal in uplift signal that may correlate with seasonal groundwater pumping during growing season

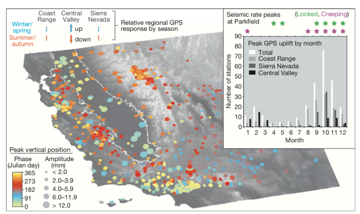

Figure 3 | Seasonal peak uplift from GPS. Phase and peak-to-peak amplitude of annual vertical GPS displacement for all stations included in our analysis. The inset shows histograms of peak uplift phase (binned by month) for stations in the San Joaquin Valley, Sierra Nevada, and Coast Range. Peaks in seismicity rate for the locked and creeping San Andreas Fault at Parkfield are defined as months with higher than average declustered seismicity[6]. Smaller-amplitude peak uplift in the Sierra Nevada and Coast Range during the dry summer and autumn is largely out of phase with larger-amplitude uplift in the San Joaquin Valley driven by the poro-elastic response to recharge during the wetter winter and spring. Stations peripheral to the valley show uplift patterns in accordance with nearby sites on bedrock, indicating the dominance of surface loads in driving vertical motions away from areas affected by local irrigation and groundwater fluctuations.

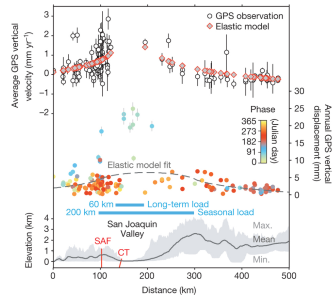

Amos et al. (2014) Nature 509

Fluid flow & the San Andreas fault

Figure 1 The San Andreas fault. The fault marks the divide between the Pacific and North American tectonic plates, and accommodates about 35 mm of the annual 48 mm of relative motion between them. The northern and southern segments last broke in major earthquakes in 1906 (magnitude 7.8) and 1857 (magnitude 8.2), respectively; the central section creeps steadily and does not accumulate strain. The other places marked are cited in the text. The physics of faulting is poorly understood, and the question of whether the San Andreas is a weak fault in a strong crust, or a strong fault in a strong crust (as Scholz[2] proposes), remains controversial. (Courtesy of the US Geological Survey.)

Zoback (2000) Nature

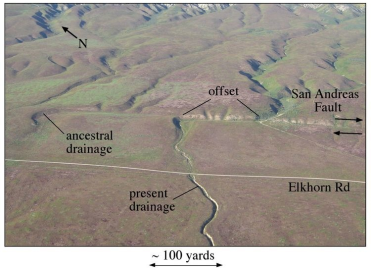

Fluid flow & San Andreas fault

- Open questions: Why are faults so weak? And why is the San Andreas fault in central California weak?
- Observations that indicate a very weak fault:
  - No frictional heat generate by rapidly moving fault
  - Creep along a large segment of the fault

Figure 1 The San Andreas fault. The fault marks the divide between the Pacific and North American tectonic plates, and accommodates about 35 mm of the annual 48 mm of relative motion between them. The northern and southern segments last broke in major earthquakes in 1906 (magnitude 7.8) and 1857 (magnitude 8.2), respectively; the central section creeps steadily and does not accumulate strain. The other places marked are cited in the text. The physics of faulting is poorly understood, and the question of whether the San Andreas is a weak fault in a strong crust, or a strong fault in a strong crust (as Scholz[2] proposes), remains controversial. (Courtesy of the US Geological Survey.)

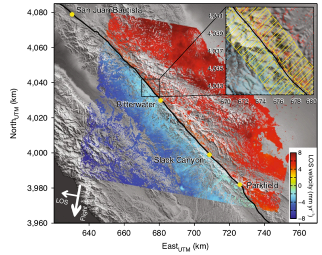

Fig. 1 | Creeping segment of the San Andreas Fault with long-term InSAR LOS velocity. The trace of the SAF is shown with the black line. Warm and cold colours correspond, respectively, to the movement towards and away from the descending satellite. The inset depicts the moving window (yellow boxes) used for estimation of near-field creep rate, with every other step shown with a lower opacity for visualization purposes. Shaded relief topography is the digital elevation model from the Shuttle Radar Topography Mission. UTM, Universal Transverse Mercator coordinate system.

Khoshmanesh (2018) Nature Geosc.

Fluid flow & San Andreas fault

- The high rate of motion along the fault should create a lot of friction and high temperatures and heat flow in the fault zone. However, measurements do not show this
- Cause:
  - Weak fault? (less friction than expected)
  - or fluid flow masking the frictional heat generated by the fault zone?

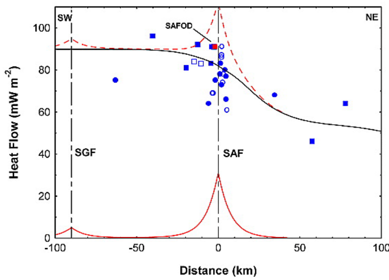

Model prediction of heat flow (broken red line) heat flow anomaly (red line) vs observed heat flow (dots) around the San Andreas fault (at distance = 0 km)
Williams et al. (2004) GRL 31(15)

Pore pressure & fault strength

- The most popular model by Rice (1992) assumes high pore pressure in the fault core in the San Andreas fault, and perhaps most large fault systems
- Overpressure due to compaction of fault core by tectonic stress
- However, many questions remain:
  - How is overpressure maintained over the earthquake cycle?
  - Is permeability sufficiently low to maintain a local pocket of overpressure without the fluid pressure diffusing outwards?
  - Do we need additional sources of fluid to maintain overpressure? If yes, where do they come from? Metamorphic dehydration reactions?

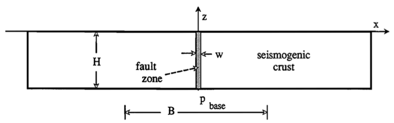

Figure 5. Cross-section of the seismogenic crust; *B* denotes the width over which elev pressures are assumed to be present.

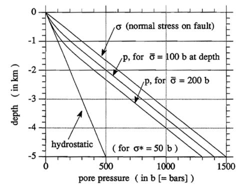

Figure 6. Pore pressure versus depth in fault zone for first 5 km of 15 km seismogenic thickness. The pore pressure distribution adjusts so that the effective normal stress, and thus also the permeability, becomes independent of depth. Based on permeability $k = k_0 \exp(-\bar{\sigma}/\sigma^*)$.

Friction in the San Andreas fault

- Recent measurements of fault core samples show very low coefficients of friction along a single borehole

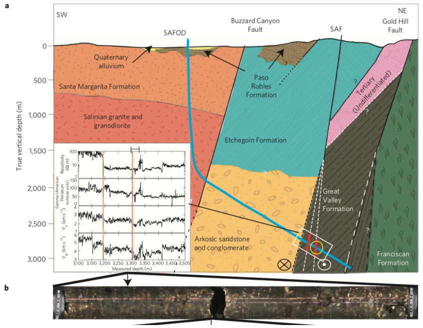

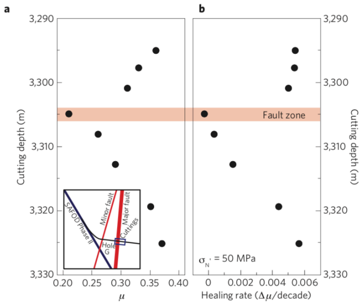

Figure 3 | Frictional strength and healing behaviour. a,**b**, Coefficient of friction (**a**) and healing rate (**b**) as a function of location across the fault zone. The frictional strength and rate of frictional healing are significantly lower in the fault zone compared with the adjacent wall rock. Inset: Schematic diagram of SAFOD boreholes in relation to the active SAF strands and the cuttings studied here.

Carpenter et al. (2011) Nature

Fault gouge clays

- Recently discovered clay gouge in the San Andreas fault: saponite (= part of smectite group clays)
- Result of fluid-assisted reaction between feldspar in host rock and serpentenite in the fault rock
- Potential cause for the anomalous low strength of the San Andreas fault
- However, weak fault rocks may not be everywhere along the fault
- And coefficient of friction can in fact increase by frictional heating (earthquakes), or decrease -> currently under debate

Lockner et al. (2011) Nature

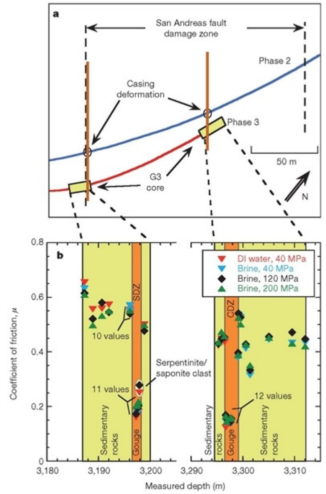

Figure 1 | Location and strengths of SAFOD core samples. a, Map view of SAF damage zone and SAFOD boreholes from phase 2 (blue) (indicating actively deforming casing) and phase 3 Hole G (red) with location of recovered core (yellow) at approximately 2.7 km vertical depth. Active deformation zones are shown in orange. **b**, Frictional strength of core samples plotted versus measured depth along Hole G (at sliding rate $V = 1.15\ \mu m\ s^{-1}$). Active fault traces SDZ (3,196.4–3,198.1 m measured depth) and CDZ (3,296.6–3,299.1 m) have notably low strength. A few samples were tested with deionized (DI) water. Extrapolation to SAF plate rate reduces shear zone strength to $\mu \approx 0.15$.

San Andreas & pore pressure

- However recent insar data show that the rate of creep along the fault varies strongly in time and space
- The most likely explanation is variation in normal stress and pore pressure over time (?)

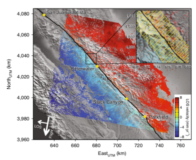

Fig. 1 | Creeping segment of the San Andreas Fault with long-term InSAR LOS velocity[20,25]. The trace of the SAF is shown with the black line. Warm and cold colours correspond, respectively, to the movement towards and away from the descending satellite. The inset depicts the moving window (yellow boxes) used for estimation of near-field creep rate, with every other step shown with a lower opacity for visualization purposes. Shaded relief topography is the digital elevation model from the Shuttle Radar Topography Mission. UTM, Universal Transverse Mercator coordinate system.

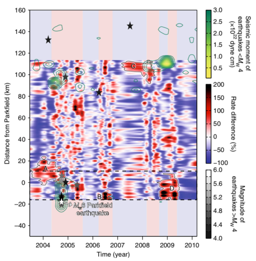

Fig. 2 | Spatiotemporal distribution of rate difference and seismicity. The relative difference between short-term (between consecutive time steps) and long-term LOS creep rate (slope of the cumulative time series) in percentage, along with moment released for earthquakes $<M_w$ 4 (green contours). Greyscale stars show the location and time of the earthquakes $>M_w$ 4. The light red and blue bands on the neighbouring segments highlight the time intervals of SSEs and the decelerated creeping, respectively. The dashed rectangle shows the approximate location of the Parkfield transition zone, which is excluded from our analyses. The areas indicated by capital letters show the extent of the significant local bursts that are discussed in the main text.

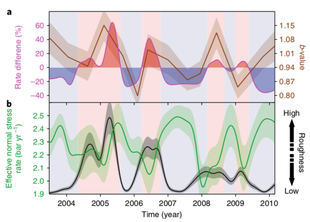

Fig. 3 | Temporal evolution of creep rate, effective normal stressing rate, roughness and *b*-value. a, Time series of spatially averaged LOS creep rate difference in percentage (magenta) and *b*-value (brown) alongside its one-sigma uncertainty (shaded brown). Background red and blue bands highlight the time interval of SSEs and decelerated creeping, respectively. **b**, Temporal evolution of spatially averaged effective normal stress rate (green) and its standard deviation (shaded green), and roughness amplitude of LOS creep rate difference along the fault (black) and its one-sigma uncertainty (shaded grey). All the curves in this figure, except the *b*-value, are smoothed using a Gaussian smoothing filter with a window size of six months.

Khoshmanesh (2018) Nature Geosc.

Summary

- Deformation of the earth's crust strongly affects fluid flow
- However, fluid flow and in particular pore pressure may play a key role in deformation
- Fractures & faulting are highly dependent on pore pressure as indicated by lab experiments and summarized by the Mohr-Coulomb failure criterion
- Case studies show correlations between seismicity, flexural uplift and groundwater recharge and pumping. Which argues for a role of pore pressure in deformation
- Case studies show that the role of fluid flow in seismic and aseismic deformation still unclear and under debate, even for well studied systems like the San Andreas fault